SECOND EUROPEAN CONFERENCE ON EARTHQUAKE ENGINEERING
AND SEISMOLOGY, ISTANBUL AUG. 25-29, 2014

DEGRADATION PARAMETERS FOR EQUIVALENT SDOF SYSTEMS OBTAINED FROM CYCLIC PUSHOVER ANALYSIS AND PARAMETER OPTIMIZATION

David KAMPENHUBER[1] and Christoph ADAM[2]

ABSTRACT

Assuming that the global hysteretic response of a planar multi-story frame structure can be represented by an equivalent single-degree-of-freedom (SDOF) system, in this study material deterioration parameters for the simplified assessment of the seismic collapse capacity are identified based on cyclic pushover analyses. Using different horizontal load pattern, global hysteretic curves of the frame structure are recorded. Given target hysteretic behavior and model properties, an equivalent SDOF system with unknown material deterioration parameters is built. Subsequent optimization analysis yields deterioration parameters that represent "optimally" the given hysteretic response of the structure. Through a parametric study varying the number of stories, the first mode period, the deterioration model and the applied load pattern for the cyclic pushover analysis, a set of equivalent deterioration parameters for the SDOF domain is identified. As an outcome a relationship between the deterioration parameters of the equivalent SDOF system and the corresponding frame structure is presented. These results allow a priori selection of deterioration parameters for the equivalent SDOF system without performing a cyclic pushover analysis on the corresponding structural frame model for simplified assessment of the seismic collapse capacity.

INTRODUCTION

Prediction with a certain confidence of the seismic intensity that may lead to earthquake induced structural collapse is one of the primary objectives of earthquake engineering. Despite the tremendous progress achieved in the last two decades through intense research, realistic collapse assessment is still a challenging task. Nowadays nonlinear dynamic analysis is the most accurate and most general tool for collapse assessment. It requires realistic modeling of the hysteretic behavior, appropriate representation of the expected modes of collapse, careful ground motion selection, consideration of modeling uncertainties, and a stable numerical algorithm, among others. In the initial design state of the structure, through the efforts required for modeling and computation, this approach is however not time efficiently applicable. Hence, there is a need for methodologies for realistic estimates of the seismic collapse capacity that are simple to apply and simultaneously sufficiently accurate.

In Adam and Jäger (2012b) such a methodology is proposed for predicting the seismic collapse capacity of highly inelastic regular moment resisting frame structures that are vulnerable to the destabilizing effect of gravity loads acting through lateral displacements (P-delta effect). The ingredients of the methods are an equivalent single-degree-of-freedom (SDOF) system of the structure, and so-called collapse capacity spectra. In a collapse capacity spectrum the collapse capacity

[1] PhD candidate, University of Innsbruck, Innsbruck, Austria, david.kampenhuber@uibk.ac.at
[2] Professor, Dr.techn., University of Innsbruck, Innsbruck, Austria, christoph.adam@uibk.ac.at

of a P-delta vulnerable SDOF system with non-deteriorating cyclic behavior is represented as a function of the initial period of vibration for a fixed set of characteristic parameters, i.e., negative post-yield stiffness ratio, damping ratio, and hysteretic loop (Adam and Jäger, 2012a; Jäger and Adam, 2013). This methodology can be applied to structures that exhibit a negative post-yield stiffness ratio with negligible material deterioration. In a first step, the actual multi-degree-of-freedom (MDOF) structure is transformed into the corresponding equivalent SDOF system. In the second step, the collapse capacity can be determined using the provided collapse capacity spectra without dynamic response history analysis. For details it is referred to Adam and Jäger (2012b). In reality, however, P-delta induced seismic sidesway collapse comes to a certain extent always along with component deterioration. According to Krawinkler et al. (2009) sidesway collapse of a structural building subjected to serve earthquake excitation is the consequence of successive reduction of the lateral load carrying capacity resulting from stiffness and strength deterioration until the global P-delta effect takes over. Depending on the structural configuration and earthquake characteristics stiffness/strength deterioration or P-delta may primarily govern seismic structural failure. Kampenhuber and Adam (2013) demonstrated the effect of material deterioration on the collapse capacity of P-delta vulnerable SDOF systems, and they proofed that for certain parameter combinations component deterioration effects may in principle not be neglected. Consequently, Kampenhuber and Adam (2013) have adopted collapse capacity spectra to include also material deterioration.

The extension of the collapse capacity spectrum methodology to P-delta sensitive frame structures that exhibit during severe seismic excitation non-negligible material deterioration requires additional information about the constitutive structural behavior. In particular, the material deterioration parameters of the MDOF system must be translated into the domain of the equivalent SDOF system. Consequently, the objective of the present paper is to identify these parameters for equivalent SDOF systems through optimization based on outcomes of cyclic pushover analyses. The underlying idea, to obtain deterioration parameter for an equivalent SDOF system through an optimization step based on a cyclic pushover analysis can also be found in Graziotti et al. (2013) and Chintanapakdee and Jaiyong (2012).

STRUCTURAL SYSTEM AND MATERIAL MODELING

For several case studies the equivalent material deterioration parameters of various generic multi-story frame structures are identified that are similar to the ones presented in Medina and Krawinkler (2003). All stories of the considered moment-resisting single-bay frame structures of N stories (N = 3, 4, 5, …, 20, respectively) are of uniform height $h = 3.66$ m, and they are composed of rigid beams and elastic flexible columns. According to the weak beam-strong column design philosophy inelastic rotational springs are located at both ends of the beams and at the base, as shown exemplarily in Figure 1. To these springs, which exhibit a bilinear backbone curve, a deteriorating bilinear cyclic model is assigned. The strength of the springs is tuned such that yielding is initiated simultaneously at all spring locations in a static pushover analysis (without gravity loads) under a first mode design load pattern. To each joint of the frames an identical point mass $m_i/2 = m_S/2$, $i = 1\ldots,N$, is assigned. The

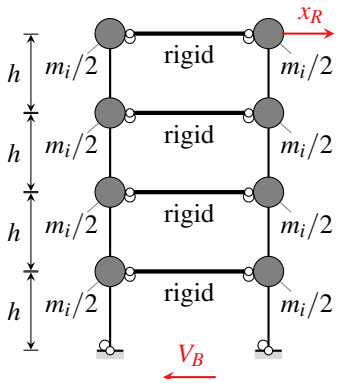

Figure 1 Mechanical modeling of the considered generic multi-story frame structures

bending stiffness of the columns and the initial stiffness of the springs are tuned to render a straight-line fundamental mode shape. The fundamental period T_1 of the frame structures and the number of stories N are related via

$$T_1 = \tau N \ , \ \tau = 0.10,\ 0.13,\ 0.16 \text{ and } 0.20 \tag{1}$$

Parameter τ quantifies the global stiffness of the frame. According to Ibarra and Krawinkler (2005) periods $T_1 = 0.10N$ and $T_1 = 0.20N$, respectively, are a reasonable lower and upper boundary for moment resisting frames. In the present investigation a bilinear backbone curve is assigned to all rotational springs of the frame. I.e., a linear elastic branch of deformation is followed by a linear inelastic range with reduced stiffness, expressed through the hardening coefficient $\alpha = 0.03$, which represents the ratio of inelastic to elastic stiffness. It is assumed that the hysteretic response of the springs is bilinear. Component deterioration is simulated with the modified Ibarra-Medina-Krawinkler deterioration model. For details on this deterioration model it is referred to Ibarra and Krawinkler (2005) and Lignos (2008). In this model the prime parameter for cyclic stiffness and strength deterioration is the dissipated hysteretic energy expressed in terms of the variable β_i,

$$\beta_i = \left(\frac{E_i}{E_t - \sum_{j=1}^{i} E_j} \right)^c \tag{2}$$

E_t represents the hysteretic energy dissipated in the *i*th inelastic excursion, $\sum_{j=1}^{i} E_j$ is the hysteretic energy dissipated in all previous excursions through loading in both positive and negative direction, and the hysteretic energy dissipation capacity

$$E_t = \Lambda M_y \tag{3}$$

is controlled by deterioration parameter Λ and the driving internal force M_y. It is assumed that E_t is an inherent property of the components regardless of the loading history applied to the component (Lignos and Krawinkler, 2011). Λ can be defined independently for acceleration reloading stiffness deterioration (then denoted as Λ_A), unloading stiffness deterioration (Λ_K), cyclic strength deterioration (Λ_S), and post-capping strength deterioration (Λ_C). Since the present study considers components with bilinear hysteretic behavior only, the acceleration reloading stiffness deterioration mode (Λ_A) does not exist. Furthermore, post-capping strength deterioration (Λ_C) is omitted, and has, thus, no influence on the results. Exponent c controls the rate of deterioration of the evaluated hysteretic parameter. According to Rahnama and Krawinkler (1993) c is a non-dimensional quantity between 1.0 and 2.0. Exemplarily shown for strength deterioration, material deterioration in the i th inelastic excursion is governed by

$$\overline{f}_{s,i} = \left(1 - \beta_{S,i}\right) \overline{f}_{s,i-1} \tag{4}$$

In this equation, $\overline{f}_{s,i}$ denotes the yield strength after the *i*th excursion, and $\overline{f}_{s,i-1}$ is the yield strength before this excursion. $\beta_{S,i}$ is the corresponding strength deterioration coefficient as defined in Eq. (2).

Upfront deterioration parameters Λ_S and Λ_K are assigned to the rotational springs of the generic frame models. In the present study each rotational spring of a specific structure exhibits the same deterioration parameters. Based on the classification of Ibarra and Krawinkler (2005) and calibration of the modified Ibarra-Medina-Krawinkler material model to experimental results (Lignos, 2008; Lignos and Krawinkler, 2011), nine different deterioration parameter sets (denoted as D_1 to D_9) as listed in Table 1 are utilized. Parameter sets D_1 to D_3 describe unloading stiffness deterioration only, sets D_4 to D_6 strength deterioration only, and sets D_7 to D_9 model simultaneous stiffness and

Table 1. Material deterioration parameters of the generic frame structures

Acronym	Type of deterioration	Deterioration speed	Λ_K	Λ_S
D_1	unloading stiffness deterioration	slow	2.0	∞
D_2	unloading stiffness deterioration	medium	1.0	∞
D_3	unloading stiffness deterioration	rapid	0.5	∞
D_4	cyclic strength deterioration	slow	∞	2.0
D_5	cyclic strength deterioration	medium	∞	1.0
D_6	cyclic strength deterioration	rapid	∞	0.5
D_7	unloading stiffness deterioration and cyclic strength deterioration	slow	2.0	2.0
D_8	unloading stiffness deterioration and cyclic strength deterioration	medium	1.0	1.0
D_9	unloading stiffness deterioration and cyclic strength deterioration	rapid	0.5	0.5

cyclic strength deterioration. In the following deterioration parameters Λ_K and Λ_S are aggregated to vector $\boldsymbol{\Lambda} = \left[\Lambda_K, \Lambda_S\right]^T$.

EQUIVALENT SINGLE-DEGREE-OF-FREEDOM SYSTEM

If the fundamental mode dominates the global hysteretic response of the considered class of MDOF structures, it is reasonable to assume that a corresponding equivalent SDOF system represents sufficiently accurate the dynamic response of the actual structure. The transformation of the model properties of the MDOF system into the domain of the equivalent SDOF system is based on a time independent shape vector $\boldsymbol{\psi}$ that describes the shape of displacement vector $\mathbf{x}$ of the MDOF structure regardless of its magnitude

$$\mathbf{x} = \boldsymbol{\psi} x_R, \quad \psi_R = 1.0 \tag{5}$$

Shape vector $\boldsymbol{\psi}$ should approximate the fundamental mode. Consequently, the only remaining degree-of-freedom is the roof displacement x_R. Furthermore, it is assumed that the shape of the backbone curve of the equivalent SDOF system is affine to the global pushover curve of the MDOF structure disregarding vertical loads. The lateral pushover load $\mathbf{F}$ is affine to the shape vector $\boldsymbol{\psi}$,

$$\mathbf{F} = \boldsymbol{\psi} F_R \tag{6}$$

Then, the displacement coordinate D^* and the base shear V_B^* of the equivalent SDOF system are both related to the corresponding quantities of the MDOF structure, i.e. the roof displacement x_R and the base shear V_B of pushover curve, through the same coefficient Γ (Fajfar, 2002),

$$D^* = \frac{x_R}{\Gamma}, \quad V_B^* = \frac{V_B}{\Gamma} \quad \text{with} \quad \Gamma = \frac{\sum_{i=1}^{N} m_i \psi_i}{\sum_{i=1}^{N} m_i \psi_i^2} = \frac{\sum_{i=1}^{N} \psi_i}{\sum_{i=1}^{N} \psi_i^2} \tag{7}$$

ψ_i is the i th component of shape vector $\boldsymbol{\psi}$. The elastic and inelastic stiffness K_e^* and K_i^*, respectively, yield strength V_{By}^*, yield displacement D_y^*, and equivalent hardening coefficient α_S^* is identified from a bilinear approximation of the global pushover curve that has been transformed into to domain of the equivalent SDOF system depicted in Figure 2.

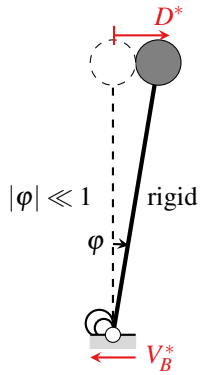

Figure 2. Mechanical modeling of the considered SDOF system

From the characteristic yield parameters of the bilinear approximation of the backbone curve the period of the equivalent SDOF system can be derived as

$$T^* = 2\pi\sqrt{\frac{L^* D_y^*}{V_{By}^*}}\,, \quad L^* = \sum_{i=1}^{N} m_i \psi_i = m_S \sum_{i=1}^{N} \psi_i \tag{8}$$

Details of the utilized equivalent SDOF system can be found in Fajfar (2002). In a further step a hysteretic law is assigned to the equivalent SDOF system. The identification of the unknown deterioration parameters Λ_K^* and Λ_S^* that govern the energy dissipation capacity (Eq. (3)) of the equivalent SDOF model is the main objective of this paper and discussed subsequently.

CYCLIC PUSHOVER ANALYSIS AND OPTIMIZATION PROCEDURE

Filiatrault et al. (2008) reviews and compares existing numerical loading protocols that have been developed for the quasi-static cyclic testing of structural components and systems. Based on this review and on numerical studies in Filiatrault et al. (2008) a cyclic loading protocol has been proposed for quantifying building system performance. Loading protocol (*A*) according to Table 2 is mainly based on this proposal und utilized for the present study. Slightly modified loading protocols (*B*) and (*C*) as defined in Table 2 are used to quantify the influence of the loading protocol on the parameter optimization. As an example, in Figure 3 loading protocol (*A*) is graphically displayed. As specified in Table 2 the load amplitude is present as a ratio of the yield roof displacement x_{Ry} of the multi-story frame structure.

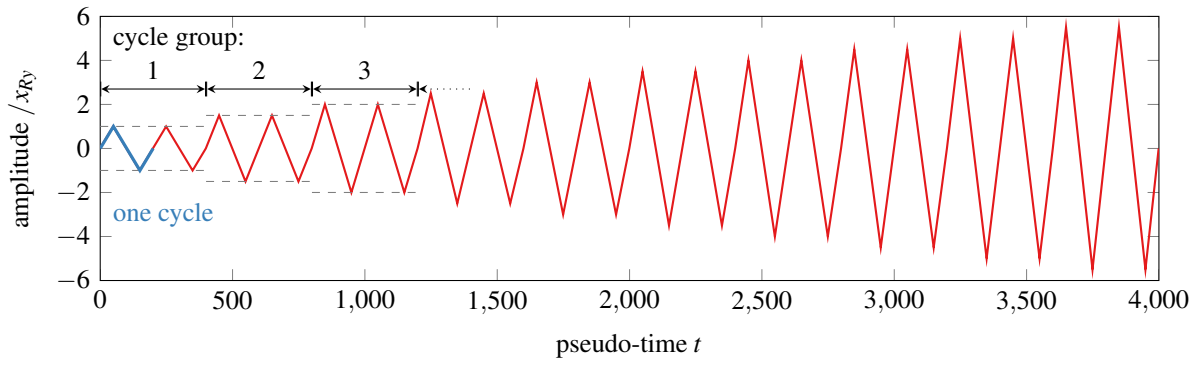

Figure 3 Loading Protocol *(A)*

Table 2. Proposed cyclic loading protocols (*A*), (*B*), and (*C*)

(*A*)	cycle group	1	2	3	4	5	6	7	8	9	10				
	n cycles	2	2	2	2	2	2	2	2	2	2				
	amplitude/ x_{Ry}	1.0	1.5	2.0	2.5	3.0	3.5	4.0	4.5	5.0	5.5				
(*B*)	cycle group	1	2	3	4	5	6	7	8	9	10	11			
	n cycles	2	2	2	2	2	2	2	2	2	2	2			
	amplitude/ x_{Ry}	1.0	1.5	2.0	2.5	3.0	4.0	3.0	2.5	2.0	1.5	1.0			
(*C*)	cycle group	1	2	3	4	5	6	7	8	9	10	11	12	13	14
	n cycles	3	3	3	3	3	3	3	3	3	3	3	3	3	3
	amplitude/ x_{Ry}	0.5	1.0	0.5	1.5	1.0	2.0	1.5	2.5	2.0	3.0	2.5	3.5	3.0	4.0

Cyclic pushover analyses are performed on each considered MDOF system. The base shear V_B is recorded at discrete time instants and collected in vector $\hat{\mathbf{y}}$. $\hat{\mathbf{y}}$ is the target vector for the optimization process of the equivalent SDOF system. With known model properties of the equivalent SDOF system, the time history of the target displacement D^* and the target time history of base shear V_B^* (whose discrete values are aggregated in vector $\mathbf{y}$), the cost function with unknown deterioration parameter vector $\mathbf{\Lambda}^* = \left[\Lambda_K^*, \Lambda_S^*\right]$ can be formulated as

$$F = \left|\left|\mathbf{y}(\mathbf{\Lambda}^*) - \hat{\mathbf{y}}(\mathbf{\Lambda})\right|\right| \rightarrow \min \tag{9}$$

$||\cdot||$ indicates the 2-norm of the vector. F is then minimized using the *Nelder-Mead simplex algorithm*, which is a direct search method without numerical or analytic gradients. Performing this optimization step for all frame structures with $N = 3,4,5,\ldots,20$ stories, respectively, fundamental periods $T_1 = \tau N$ according to Eq. (1), hysteretic laws D_1 to D_9 (Table 1), and loading protocols (A), (B), (C) (Table 2) results in 1944 deterioration parameters Λ_S^*, Λ_K^* for the equivalent SDOF system.

As an example, in Figure 3 the results for a 10-story generic frame structure with $T_1 = 1.60$ s and medium deterioration in strength and stiffness (parameter set D_8) are depicted. Therein, the normalized global hysteretic response of the MDOF system (x_R vs V_B) with upfront defined deterioration parameters $\Lambda_S = \Lambda_K$ is set in contrast to the corresponding outcome of the equivalent SDOF domain (D^* vs V_B^*) but with optimized equivalent deterioration parameters Λ_S^* and Λ_K^* identified through the described optimization procedure. All depicted quantities are normalized with respect the corresponding quantities at yield initiation. Subplots (a), (b), and (c) show the structural response to loading protocols (A), (B), and (C), respectively. Degradation parameter Λ_K and Λ_S from the MDOF system and the resulting degradation parameter Λ_K^* and Λ_S^* of the equivalent SDOF system obtained through the optimization step are summarized in Table 3.

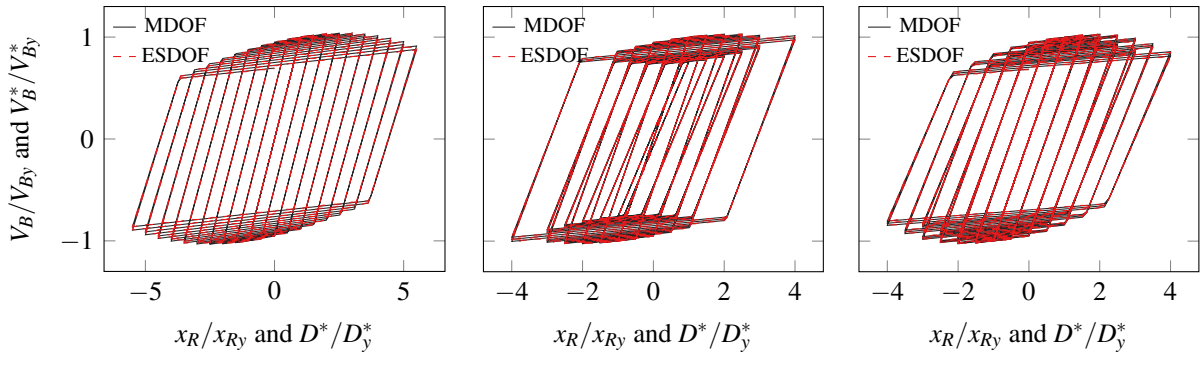

Figure 4 Normalized hysteretic response to (a) loading protocol (A), (b) (B), and (c) (C)

Table 3 Comparison of degradation parameters for the frame structure and identified degradation parameters for the equivalent SDOF system

Underlying loading protocol	MDOF system		Equivalent SDOF system	
	Λ_K	Λ_S	Λ_K^*	Λ_S^*
(A)	1.0	1.0	33.2	25.6
(B)	1.0	1.0	33.8	25.9
(C)	1.0	1.0	31.1	25.2

Evaluation of the normalized root mean square error (*NRMSE*, MATLAB, 2014),

$$c_j(\boldsymbol{\Lambda}^*) = 1 - \frac{\left\| \mathbf{y}(\boldsymbol{\Lambda}^*) - \hat{\mathbf{y}}(\boldsymbol{\Lambda}) \right\|}{\left\| \mathbf{y}(\boldsymbol{\Lambda}^*) - \text{mean}(\hat{\mathbf{y}}(\boldsymbol{\Lambda})) \right\|} \quad j = (A), (B), (C) \tag{10}$$

is used to check the accuracy of the optimized parameters. The "cost" c_j is calculated for the jth loading protocol and varies between $-\infty$ (bad fit) to 1 (perfect fit). For the previously considered 10-story structure with a fundamental period $T_1 = 1.60$s the cost is for all loading protocols close to 1, i.e., $c_{(A)} = 0.9956$, $c_{(B)} = 0.9925$ and $c_{(C)} = 0.9955$, respectively. This outcome proves that the identified deterioration parameters reflect accurately the actual behavior of the MDOF system.

OUTCOMES OF THE DETERIORATION PARAMETER IDENTIFICATION

Subsequently, in Figures 5 to 8 the ratios of the identified equivalent SDOF system deterioration parameters to the corresponding MDOF system deterioration parameters, Λ_K^* / Λ_K and Λ_S^* / Λ_S, respectively, are plotted against the fundamental period T_1, varying the deterioration speed from slow (Figure 5), medium (Figure 6) to rapid (Figure 7). Ratios for each loading protocol (A), (B), (C) respectively, are presented separately in subplots (a), (b), (c), respectively. Therein, colored markers represent the results based on a combined strength and stiffness deterioration.

In Figure 8 ratios of degradation parameter for loading protocol (B) and *medium* deterioration speed are plotted for both for single stiffness/strength deterioration (shown by gray markers) and combined strength and stiffness deterioration (shown by colored markers).

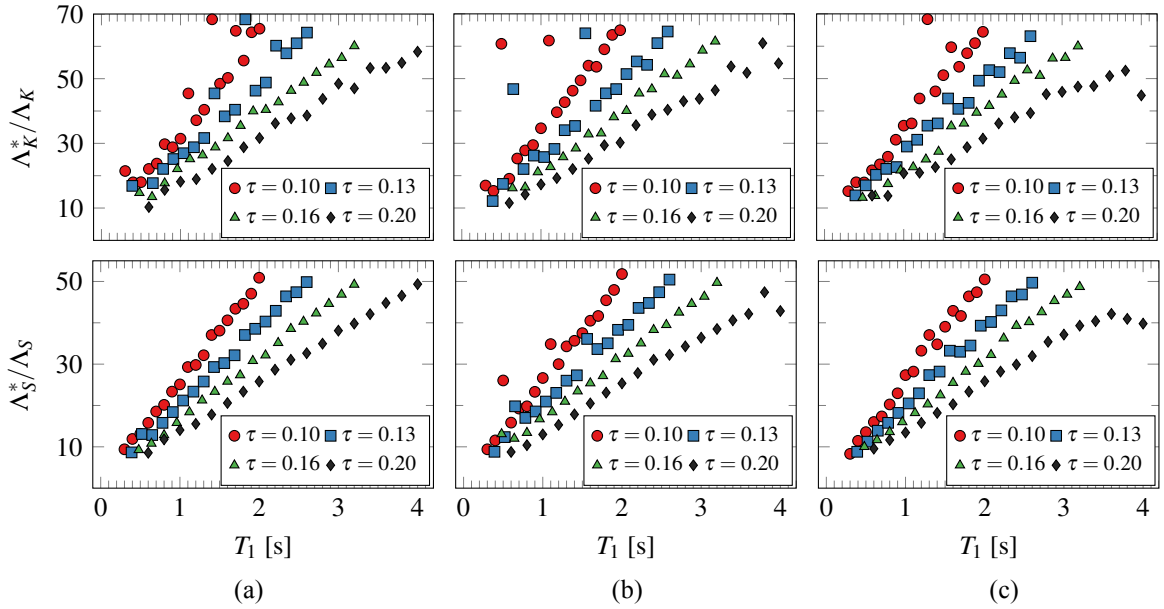

Figure 5 Deterioration parameter ratios Λ_K^* / Λ_K and Λ_S^* / Λ_S for parameter sets D_1, D_4 (gray markers) and parameter set D_7 (colored markers)

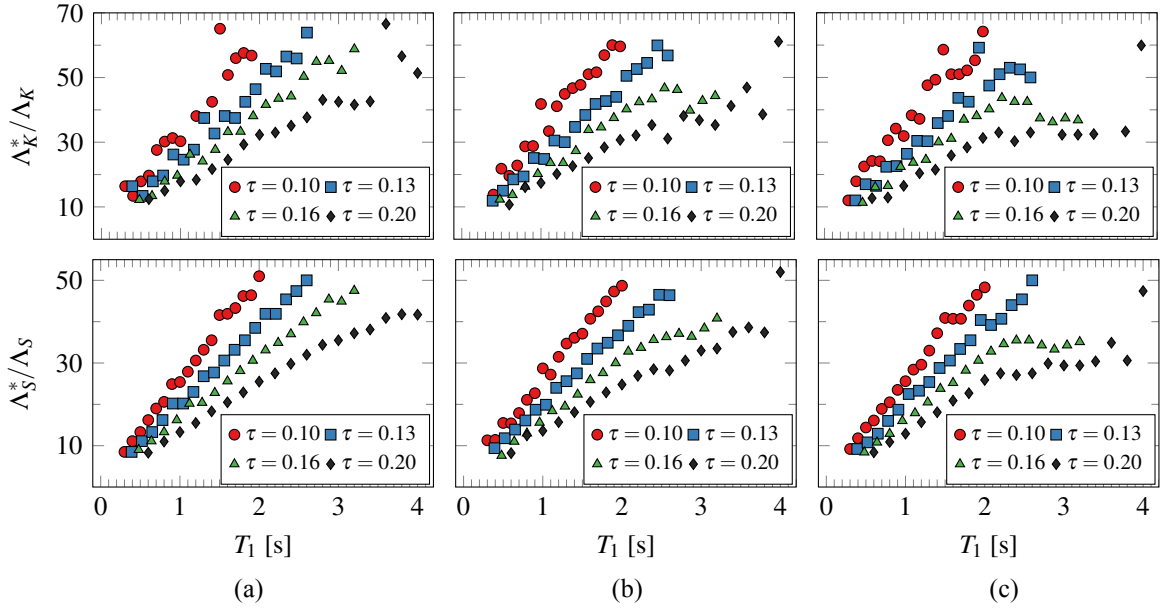

Figure 6 Deterioration parameter ratios Λ_K^* / Λ_K and Λ_S^* / Λ_S for parameter sets D_2, D_5 (gray markers) and parameter set D_8 (colored markers)

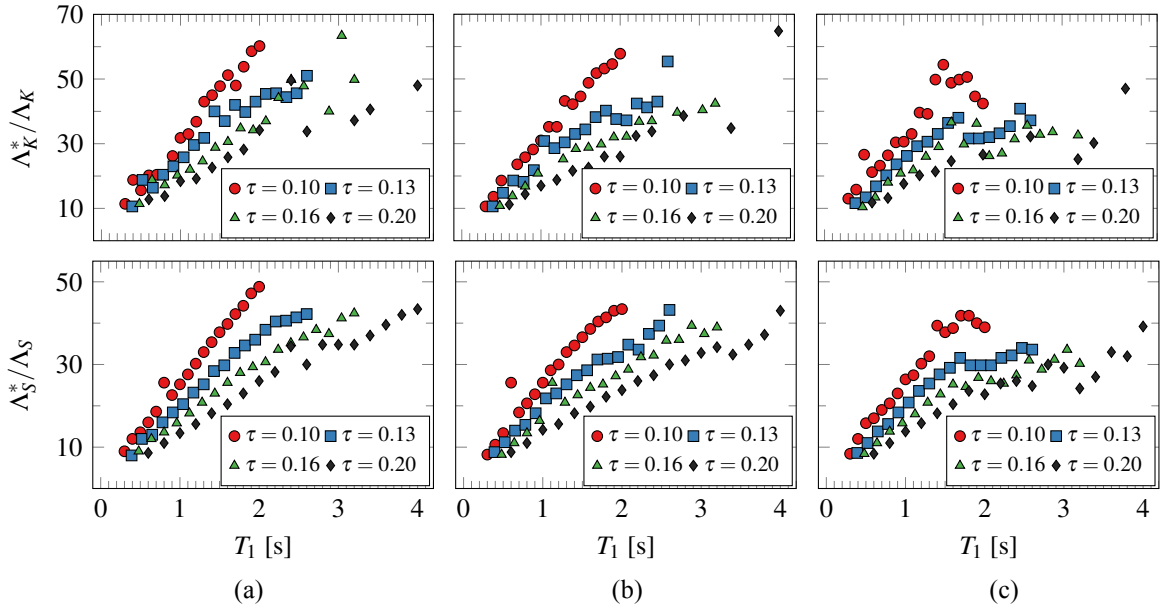

Figure 7 Deterioration parameter ratios Λ_K^* / Λ_K and Λ_S^* / Λ_S for parameter sets D_3, D_6 (gray markers) and parameter set D_9 (colored markers)

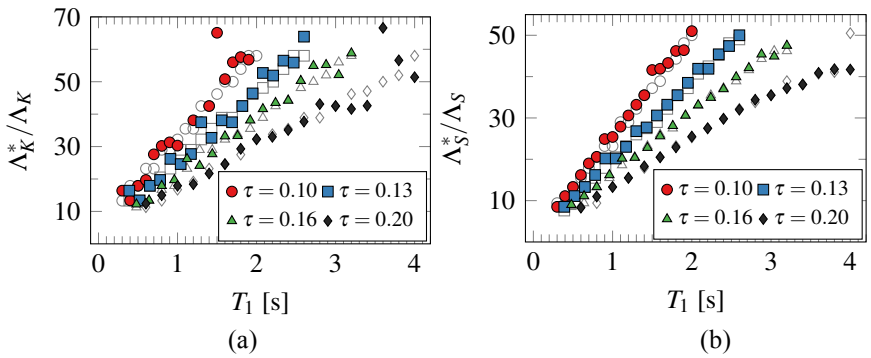

Figure 8 Deterioration parameter ratios Λ_K^* / Λ_K and Λ_S^* / Λ_S for parameter set (a) D_2 (gray markers); D_8 (colored markers) and (b) D_5 (gray markers); D_8 (colored markers)

The results of these figures show that, as supposed, the equivalent deterioration parameter of the equivalent SDOF system primarily depends on the fundamental period of the structure and less significantly on factor τ that relates period T_1 and story number N. Inspection the subplots (a) to (c) of Figures 5 to 7 leads to the conclusion that the identified deterioration parameter is almost unaffected by the underlying loading protocol if the structural period $T_1 < 2.0$ s. For frames with slow material deterioration this holds true also for periods $T_1 \geq 2.0$ s; see Figure 5.

For long period structures ($T_1 \geq 2.0$ s) combined with medium or rapid material deterioration, the optimization procedure yields deterioration parameters that depend slightly on the loading protocol. This might be a result of a reduced accuracy of the optimization process.

The accuracy of the identified parameters is evaluated through the cost c_j according to Eq. (10), and depicted in Figure 9 for all material models D_i, $i = 1,...,9$. c_j is shown for each parameter ratio and each loading protocol (A), (B), (C) separately in subplots (a), (b), (c).

Figure 9 reveals that for slow material deterioration in almost the entire considered period range the cost is close to 1 (denoted by red markers), i.e., the response of the MDOF structure and of the equivalent SDOF system using the identified parameter set is in good agreement. Only for periods close to 4.0 s the cost values are slightly smaller than 1. However, for structures exhibiting medium and rapid material deterioration (denoted by blue markers and black markers, respectively), this error quantity starts to become smaller than 1 already for periods at about 2.0 s, see Figure 9.

In general the identified parameter set leads for all three deterioration speeds to equivalent SDOF system response predictions that are close the quasistatic response of the corresponding MDOF structure. To underline this conclusion, Figure 10 shows the time history of base shear V_B (black line) and V_B^* (red line), respectively, for two different structural configurations. For the underlying structural configuration of subplot (a), i.e., a 10 story generic frame with a fundamental period of $T_1 = 1.60$ s and medium material deterioration, the cost value is close to 1 ($c_{(C)} = 0.9955$). For the underlying structural configuration of subplot (b), i.e., a flexible 20 story structure with a fundamental period of $T_1 = 4.0$ s that exhibits rapid material deterioration, the error quantity is significantly smaller than 1 ($c_{(C)} = 0.8064$). Both structures are subjected to loading protocol (C).

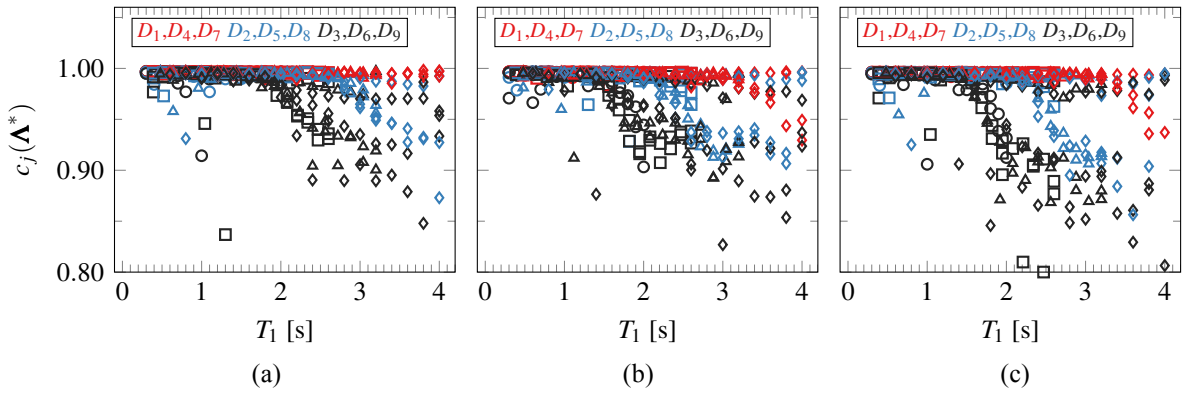

Figure 9. Quality of optimization (a) loading protocol (A) (b) loading protocol (B) (c) loading protocol (C)

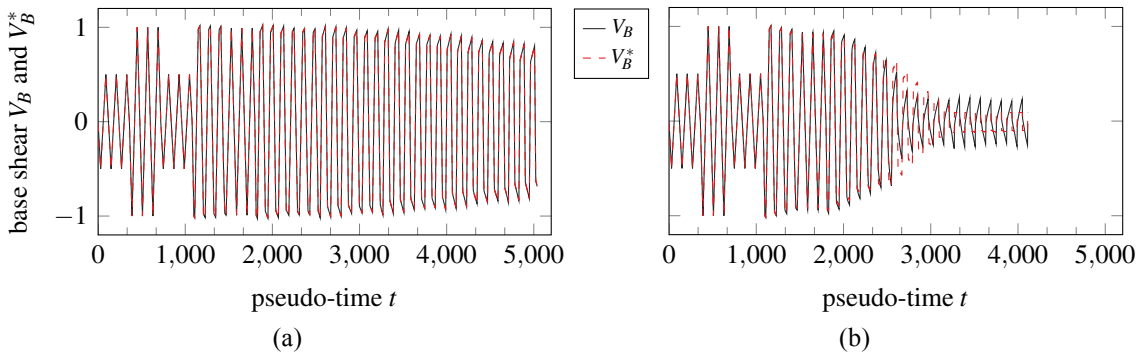

Figure 10 Comparison of $\mathbf{y}$ (red) and $\hat{\mathbf{y}}$ (black) for (a) a 10 story generic frame and (b) 20 story generic frame

It should be emphasized that the latter structural model exhibits collapse before it is subjected to the complete loading protocol (C). Consequently, the recorded response shown in Figure 10b is shorter than loading protocol (C) as listed in Table 2. Close inspection of the results reveals that for MDOF structures that are driven into a state close to collapse the deviation between the response of the frame structure and the predicted response of the equivalent SDOF system becomes more pronounced. In the MDOF structure the global hysteretic curve exhibits a smooth transition between the linear elastic branch and post-yield branch of deformation. In contrast, in an equivalent SDOF system the shape of the hysteretic loop is sharply bilinear, because the hysteretic behavior is represented by a single spring at the base only, and thus the smooth transition present in the real structure cannot be captured. This transition zone becomes more pronounced when the structure is close to collapse, and thus, the accuracy of the response approximation by an equivalent SDOF system decreases. Altogether in can be concluded that the utilized equivalent SDOF system represents the global behavior of the actual frame structure sufficiently accurate and is therefore accepted.

In the period range $0 \le T_1 \le 2.0$ s the relation between the deterioration parameter ratios Λ_K^* / Λ_K, Λ_S^* / Λ_S and the period T_1 is almost linear, and unaffected by the deterioration speed and the applied loading protocol. Factor τ, which relates the fundamental period and the number of stories, governs, however, the gradient of this relation.

ANALYTICAL APPROXIMATION OF THE EQUIVALENT DETERIORATION PARAMETERS

Given period T_1, factor τ, and deterioration parameters Λ_K, Λ_S of the MDOF structure, from Figures 5 to 8 the deterioration parameters Λ_K^*, Λ_S^* of the corresponding equivalent SDOF system can be determined without performing a cyclic pushover analysis on the MDOF model, and thus, the applicability of simplified response prediction methods such as the collapse capacity spectrum methodology remains retained. To keep these results as simple as possible, subsequently an analytical approximation of the derived empirical Λ_K^* / Λ_K and Λ_S^* / Λ_S ratios is determined trough linear regression analysis. Figure 11 grey markers represent for four different factors τ individual Λ_K^* / Λ_K and Λ_S^* / Λ_S ratios with respect to period T_1. Since some of these data are outliers, from these results median values are determined comprising all loading protocols (A), (B), and (C) and material models D_1 to D_9 through vertical statistics. In the subplots of Figure 11 colored markers depict the resulting median relations of the deterioration parameter ratios.

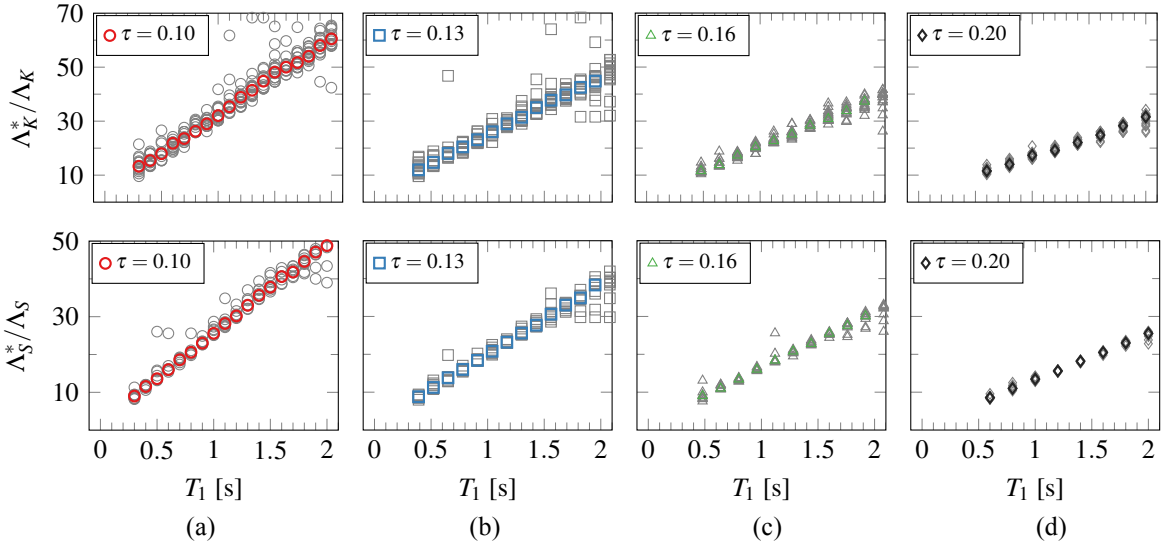

Figure 11. Median values of deterioration parameter ratios Λ_K^* / Λ_K and Λ_S^* / Λ_S

In a subsequent step linear regression analyses render for the period range $0.3\text{s} \le T_1 \le 2.0\text{s}$ a linear approximation of the median data,

$$\Lambda_{K,S} / \Lambda^*_{K,S} = aT_1 + b \tag{11}$$

as shown in Figure 12. Depending on coefficient τ in Table 4 slope a and intercept b is listed.

With given ratios Λ^*_K / Λ_K, Λ^*_S / Λ_S and known deterioration parameters Λ_K, Λ_S of the MDOF model, the equivalent deterioration parameters Λ^*_K, Λ^*_S are determined.

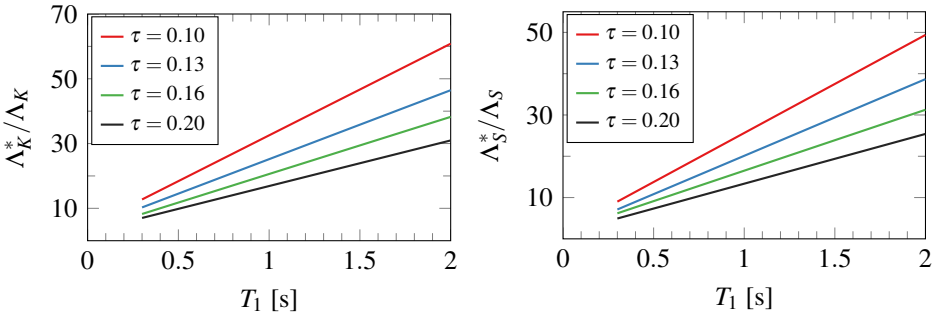

Figure 12. Regression parameter for given period T_1 and story number N

Table 4. Slope a and intercept b for the regression lines shown in Figure 12

	$\tau = 0.10$		$\tau = 0.13$		$\tau = 0.16$		$\tau = 0.20$	
	a	b	a	b	a	b	a	b
Λ^*_K / Λ_K	28.29	4.25	21.29	3.89	17.64	2.96	14.08	2.80
Λ^*_S / Λ_S	23.75	1.89	18.57	1.54	14.75	1.76	12.05	1.31

SUMMARY AND CONCLUSION

Assuming that the global hysteretic response of a generic multi-story structure can be represented by an equivalent single-degree-of-freedom (SDOF) system, in this study material deterioration parameters for the simplified assessment of the collapse capacity are identified through cyclic pushover analyses. On the basis of different sets of loading protocols, material models, structural systems with various numbers of stories and fundamental periods equivalent deterioration parameters of the Ibarra-Medina-Krawinkler material deterioration model of the equivalent SDOF system and their relation to the corresponding parameters of the underlying multi-story frame structure have been identified. From the outcomes of this study it can be concluded that the equivalent deterioration parameter primarily depend on the fundamental period of the structure, and less significantly, on a factor that relates the fundamental period and the number of stories. The identified deterioration parameters are almost unaffected by the loading protocol if the fundamental period is less than 2.0 s. For frames with slow material deterioration this holds true also for larger periods. For long period structures with fundamental periods ≥ 2.0 s, combined with medium or rapid material deterioration, the optimization procedure yields deterioration parameters that depend slightly on the loading protocol. Based on the outcomes of these parameter studies and regression analyses, analytical relations for the equivalent deterioration parameters (related to the corresponding parameters of the multi-story frame structure) are provided that allow a priori selection of deterioration parameters for the equivalent SDOF system without performing any computation, for the simplified assessment of the seismic response.

REFERENCES

Adam C, Ibarra LF, Krawinkler H (2004) "Evaluation of P-delta effects in non-deteriorating MDOF structures from equivalent SDOF systems", *Proceedings of the 13th World Conference on Earthquake Engineering*, Vancouver B.C., 1-6 August, DVD–ROM paper 15pp.

Adam C, Jäger C (2012a) "Seismic collapse capacity of basic inelastic structures vulnerable to the P-delta effect", *Earthquake Engineering & Structural Dynamics*, 41: 775-793

Adam C, Jäger C (2012b) "Simplified collapse capacity assessment of earthquake excited regular frame structures vulnerable to P-delta", *Engineering Structures*, 44: 159-173

Chintanapakdee C, Jaiyong A (2012) "Estimation of Peak Roof Displacement of Degrading Structures", *Proceedings* of the *15th World Conference on Earthquake Engineering (15WCEE),* Lisbon, 24-28 September, DVD-ROM paper 835

Fajfar P (2002) "A breakthrough of simplified nonlinear methods", *Proceedings of the 12th European Conference on Earthquake Engineering,* CD–ROM paper, Paper Ref. 843, 20 pp.

Filiatrault A, Wanitkorkul A, Constantinou MC (2008) Development and appraisal of a numerical cyclic loading protocol for quantifying building system performance, MCEER-08-0013. University at Buffalo, State University of New York: Multidisciplinary Center for Earthquake Engineering Research (MCEER).

Graziotti F, Penna A, Magenens G (2013) "Use of equivalent SDOF systems for the evaluation of displacement demand for masonry buildings", *Proceedings of the Vienna Congress on Recent Advances in Earthquake Engineering and Structural Dynamics 2013 (VEESD 2013)*, Vienna, 28-30 August, Paper No. 347

Ibarra LF, Krawinkler H (2005) Global collapse of frame structures under seismic excitations, Report No. PEER 2005/06, Pacific Earthquake Engineering Research Center, University of California, Berkeley, CA

Jäger C, Adam C. (2013) "Influence of Collapse Definition and Near-Field Effects on Collapse Capacity Spectra", *Journal of Earthquake Engineering*, 17: 859–878

Kampenhuber D, Adam C (2013) "Seismic collapse capacity of basic inelastic structures vulnerable to the P-delta effect", *Proceedings of the Vienna Congress on Recent Advances in Earthquake Engineering and Structural Dynamics 2013 (VEESD 2013)*, Vienna, 28-30 August, Paper No. 424

Krawinkler H, Zareian F, Lignos D, Ibarra LF (2009) "Prediction of collapse of structures under earthquake excitations", *Proceedings of the 2nd International Conference on Computational Methods in Structural Dynamics and Earthquake Engineering (COMPDYN 2009)*. Rhodes, 22-24. June, CD-ROM paper, Paper No CD449, 19 pp.

Lignos D (2008) Sidesway collapse of deteriorating structural systems under seismic excitations, Ph.D. thesis, Stanford University, Department of Civil and Environmental Engineering

Lignos D, Krawinkler H (2011) "Deterioration modeling of steel components in support of collapse prediction of steel moment frames under earthquake loading" *Journal of Structural Engineering*, 137(11): 1291-1302

MATLAB (2014) The MathWorks, Inc. *URL: http://www.mathworks.de/de/help/ident/ref/ goodnessoffit.html*.

Medina RA, Krawinkler H (2003) Seismic demands for nondeteriorating frame structures and their dependence on ground motions, Report No. 144. The John A. Blume Earthquake Engineering Research Center, Department of Civil and Environmental Engineering, Stanford University, Stanford, CA

OpenSees (2014) "Open system for earthquake engineering simulation", Pacific Earthquake Engineering Research Center, University of California at Berkeley, Berkeley CA. URL: http://opensees. berkeley.edu/

Rahnama M, Krawinkler H (1993) Effects of soft soil and hysteresis model on seismic demands, Report No. 108. The John A. Blume Earthquake Engineering Research Center, Department of Civil and Environmental Engineering, Stanford University, Stanford, CA